The 2014 World Congress on
Advances in Civil, Environmental, and Materials Research (ACEM14)
Busan, Korea, August 24-28, 2014

Dynamic characteristics of a base-isolated RC frame structure with and without infill walls under ambient excitation

*Jian-ping Han[1)] and Yun-shuai Liu[2)]

[1), 2)] *Key Laboratory of Disaster Prevention and Mitigation in Civil Engineering of Gansu Province, Lanzhou University of Technology, Lanzhou 730050, China*
[1)] *jphan@lut.cn*

ABSTRACT

In order to investigate the dynamic characteristics of base-isolated structures under ambient excitation, ambient vibration tests were conducted on a base-isolated RC frame structure before and after the infill walls were constructed. Modal frequencies, mode shapes and damping ratios of the investigated structure in the two cases were identified using Stochastic Subspace Identification (SSI) and Rational Fraction Polynomial (RFP) methods. Then identified modal parameters were taken as the basis to inverse the actual horizontal equivalent stiffness of isolation layer under ambient vibration by multi-objective optimization method. Inversed results show that the actual stiffness value is 10.9 times of that under frequently-occurred earthquake level for the case with infill walls, and it is 10.75 times of design value for the case without infill walls. Furthermore, damping characteristics and dynamic parameters of the base-isolated structure with the different shear deformation of rubber bearings were discussed. There is large difference of main dynamic characteristics of entire structure under different level excitations.

1. INTRODUCTION

In recent years, base isolation technology has been already applied in more and more buildings. The good performance of base-isolated structures has already been conformed by the actual strong earthquake events such as Wenchuan earthquake in China on May 12, 2008 and Tohoku Earthquake and Tsunami in Japan on March 11, 2011 (Mo et al. 2008, Kasai 2011).

The design of base-isolated structures is based on the parameters of isolators under certain shear deformation level which is supposed to be reached when the isolators are forced by prescribed levels of earthquake such as frequently-occurred earthquake and rarely-occurred earthquake according to the seismic design code (GB50011-2010). Under such cases, dynamic characteristics and performance of base-isolated

[1)] Professor
[2)] Doctoral student

structures have been investigated very well. But when the base-isolated structures work under ambient vibration or low level horizontal ground motion, the stiffness and damping of laminated rubber bearings (LRBs) and dynamic characteristics of structures are different from the design cases because the shear deformation level of the LRB is far less than the designed level. For this reason, the research on dynamic characteristics and parameters of base-isolated structures under low level ground motion and ambient vibration is still needed. Nowadays, clear conclusion on this is still not reached.

In this paper, ambient vibration tests were conducted on a base-isolated RC frame structure before and after the infill walls were constructed, respectively. The main dynamic characteristics of base-isolated structure under ambient vibration is studied and compared with dynamic parameters under frequently-occurred earthquake and rarely-occurred earthquake.

2. DESCRIPTION OF INVESTIGATED BASE-ISOLATED STRUCTURE AND INITIAL FINITE ELEMENT MODELING

The base-isolated building investigated in this paper is a 4-storey public teaching building of a primary school. It is a typical base-isolated reinforced concrete frame with LRBs in China, which is located in the region of seismic fortification intensity 8 with basic peak ground acceleration 0.2g. Overall height of the building is 15.6m. The overall views of the building with and without infill walls are shown in Fig. 1. A close-up of a positioned LRB and the horizontal isolation seam between superstructure and ground are shown in Fig. 2. The deployment of LRBs is shown in Fig. 3. And design parameters of each kind of LRB are shown in Table 1.

(a) Without infill walls (b) With infill walls and architectural coating

Fig. 1 Views of the building before and after the infill walls were constructed

Fig. 2 Close-up views of a positioned LRB and horizontal isolation seam

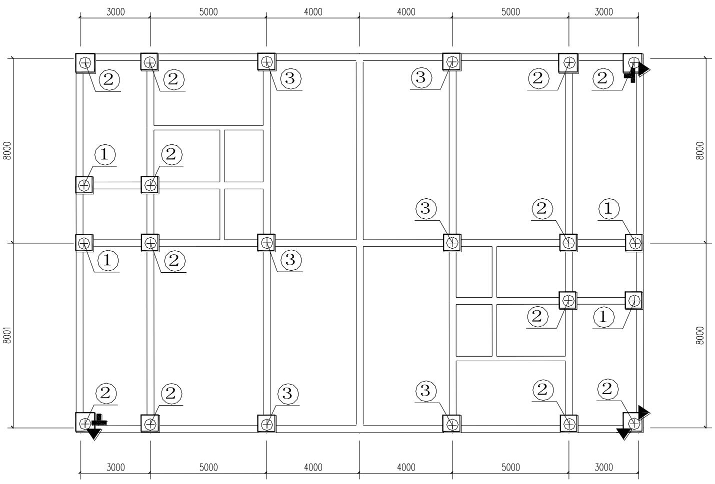
(▶ Traveling accelerometer; ┻ Reference accelerometer)

Fig. 3 LRB deployment of the tested building and accelerometer locations

Table 1 Detailed design parameters of LRBs under different shear deformation level

No	Type	$\gamma = 50\%$		$\gamma = 250\%$	
		K (kN/m)	ζ	K (kN/m)	ζ
1	GZY400	1800	0.2	820	0.15
2	GZY500	2200	0.2	920	0.15
3	GZP600	1200	0.05	1200	0.05

In order to ensure better quality of the experimental data, the initial finite element model of this base-isolated building with and without infill walls were built respectively prior to ambient vibration tests. Given that the deformation of isolation layer is small under ambient excitation, the initial stiffness of rubber bearing was taken tentatively as 10 times of the design value under frequently-occurred earthquake (Zhou 1997).

Modal analysis was performed on the two initial models. The first 3 mode frequencies of the building with infill walls are 2.886 Hz, 3.521 Hz and 6.936 Hz. For the building without infill walls, they are 2.370 Hz, 3.071 Hz and 6.838 Hz, respectively.

3. AMBIENT VIBRATION TEST AND MODAL PARAMETER IDENTIFICATION

3.1 Dynamic testing under ambient excitation

Ambient vibration test was conducted on the base-isolated structure using DASP signal acquisition and analysis system before and after the infill walls were constructed respectively. Piezoelectric acceleration sensor was used to measure the response of each gauge point. Sampling frequency is taken as 80Hz and sampling time of each set-up is taken as 20min, a total of 10 separate set-ups were selected to test. In order to lessen the influence of external interference, the tests were conducted late at night.

2 ambient vibration tests have the same accelerometer arrangement. As shown in Fig. 3, 4 unidirectional horizontal accelerometers were used on each floor, and 2

reference sensors were placed on the roof (one in each direction). Traveling accelerometers were moved one floor after another, and reference accelerometers were fixed on the roof during the test.

3.2 Modal parameter identification

In order to increase the confidence of the identification results, two independent modal parameter identification methods were used with the same data. One is Stochastic Subspace Identification (SSI) in time domain and another is Rational Fraction Polynomial (RFP) in frequency domain. The SSI method is a relatively advanced time domain method for modal identification as it can distinguish reliably between structural and operational under ambient excitation. On the other hand, the RFP method using modal expansion without any simplification and so can obtain modal parameter with good accuracy (Overschee and Moor 1996, Juang 1994, Han et al. 2008).

Recorded X, Y-direction data of gauge points were adopted to identify modal parameters. The identified results of modal parameters are shown in Table 2. Frequencies of the structure with infill walls are larger than the values of the structure without infill walls. But the identified mode shapes of the structure with and without infill walls are essentially identical. Fig. 4 shows the identified first 3 mode shapes of the structure with infill walls.

Table 2 Identification results of modal parameters

Mode No.	Building with infill walls					Building without infill walls				
	SSI		RFP		MAC	SSI		RFP		MAC
	ω_i (Hz)	ζ_i (%)	ω_i (Hz)	ζ_i (%)		ω_i (Hz)	ζ_i (%)	ω_i (Hz)	ζ_i (%)	
1	3.0666	1.29	2.9908	2.05	0.96	2.5672	2.18	2.5713	5.71	0.91
2	3.9061	3.26	3.9022	2.28	0.89	3.2810	1.08	3.2831	3.21	0.85
3	6.3809	1.52	6.1849	3.89	0.94	6.1824	2.04	6.2018	2.26	0.84
4	8.2285	1.86	8.1756	3.21	0.86	7.7110	2.30	7.7909	1.24	0.81
5	9.7962	4.39	8.9563	5.59	0.77	8.370	0.50	8.501	1.22	0.81
6	13.334	6.86	12.012	4.22	0.79	12.710	2.01	11.776	5.04	0.78

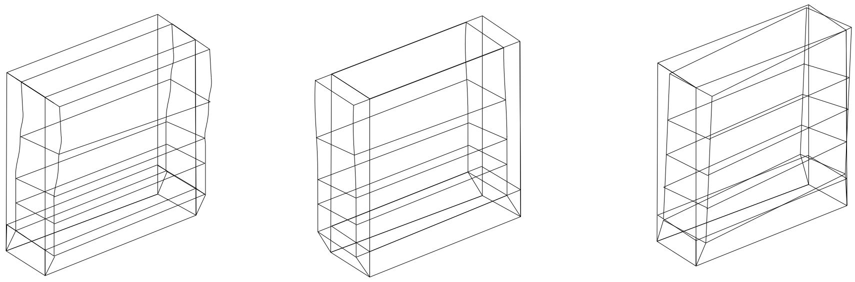

(a) 1st transverse (b) 1st longitudinal (c) 1st torsion

Fig. 4 Identified first 3 mode shapes of the structure with infill walls

The correlation between the identified modes from SSI and RFP can be quantified using modal assurance criterion (MAC). MAC values were also shown in Table 2 and the minimum one is 0.77. This result indicates that there is a good correlation between the two methods and these two methods are reliable and practical.

3.3 Discussion on the identified damping ratios

In engineering applications of current stage, damping of the structures without isolation is often assumed to be proportional damping. And the damping of the based-isolated structures is generally regarded as non-proportional damping because there is a big difference of damping characteristics between isolation system and the superstructure (Du et al. 2003). But as shown in Table 2, the damping ratios of the identified modes are all relatively small under ambient excitation. The equivalent damping ratios of base-isolated structures are very close to the values of base-fixed structures. The main reason is that when the rubber bearing is subjected to low level vibration such as ambient excitation, its displacement and strain induced by lateral vibration are all rather small, thus the energy dissipation of the rubber bearing is very small. So the isolation layer contributes less to the overall damping under low level vibration than under moderate and strong vibration (Ventura et al. 2003).

Recorded velocity time histories of two gauge points at top and bottom of a rubber bearing are shown in Fig. 5. Absolute velocity values of both two points are very small and relative velocity value of the rubber bearing is also very small. So the damping that provided by rubber bearing is rather low necessarily.

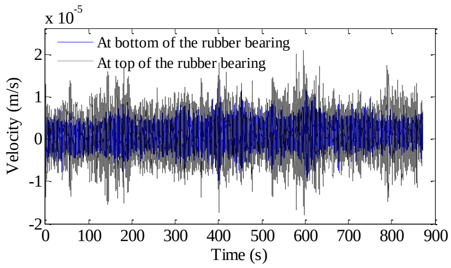

Fig. 5 Velocity time histories at top and bottom of a rubber bearing in the case without infill walls

Although the damping mechanism of rubber bearing is different from the superstructure, damping characteristic they behave under ambient excitation does not have too much difference. For this reason, the base-isolated structure is treated as a classically proportional damped system in further study.

4. INVERSION OF ACTUAL HORIZONTAL STIFFNESS OF ISOLATION LAYER UNDER AMBIENT EXCITATION

As discussed above, the isolators provide an almost fixed connection between the superstructure and substructure under ambient excitation. The shear strain of rubber bearing is far less than the supposed values under frequently-occurred earthquake and rarely-occurred earthquake. So the dynamic characteristics of base-isolated structures under ambient excitation would quite differ from the design cases. In order to investigate fully the dynamic characteristics of base-isolated structures under low-amplitude excitation such as ambient excitation, to determine the actual horizontal stiffness of isolation layer reasonably is necessary. In this paper, the multi-objective optimization method based on the identified results under ambient excitation was used for inverting the actual horizontal stiffness of the isolation layer. In order to improve the reliability of optimization processes, the same multi-objective optimization processes were separately conducted for the cases with and without infill walls. As discussed above, the story shear model with proportional damping was used to simulate numerically the base-isolated structure.

Taking structure with infill walls as an example, modal analysis was conducted on the built model to obtain analytical frequencies and mode shapes. Then the sum squared error of the first 3 identified and analytical mode frequencies and the negative value of MAC of the first 3 modes were taken as objective functions. The mathematical model of multi-objective optimization was established as the following:

$$\min\left\{f\left(k_{\mathrm{b}}\right)\right\}=\left\{\begin{array}{c}\sum_{i=1}^{3}(\omega_{\mathrm{e}i}-\omega_{\mathrm{a}i})^{2}\\ \sum_{i=1}^{3}\left(1-\frac{(\phi_{\mathrm{a}i}^{\mathrm{T}}\phi_{\mathrm{e}i})^{2}}{(\phi_{\mathrm{a}i}^{\mathrm{T}}\phi_{\mathrm{a}i})(\phi_{\mathrm{e}i}^{\mathrm{T}}\phi_{\mathrm{e}i})}\right)\end{array}\right\}\qquad(i=1,2,3)\tag{1}$$

$$\begin{array}{ll} s.t. & [M]\{\ddot{x}\}+[K]\{x\}=0\\ & [K]\{\phi_{\mathrm{a}i}\}=[M]\{\phi_{\mathrm{a}i}\}\omega_{i}^{2}\qquad(i=1,2,3)\end{array}\tag{2}$$

where $\omega_{\mathrm{e}i}$ and $\phi_{\mathrm{e}i}$ are identified frequency and mode shape vector of the i^{th} mode based on ambient vibration test, $\omega_{\mathrm{a}i}$ and $\phi_{\mathrm{a}i}$ are analytical frequency and mode shape vector of the i^{th} mode. k_{b} is horizontal stiffness of isolation layer. $[M]$ and $[K]$ are mass and stiffness matrix of the system respectively.

In order to optimize the objective functions as a whole, the linear weighted sum method was used. The squared error objective functions of frequencies and negative MAC objective functions of the first 3 mode shapes were multiplied by different weighting coefficients $\gamma_i\ (i=1,\ 2,3)$ respectively. So objective functions were converted as the following:

$$\begin{array}{l} f\left(k_{\mathrm{b}}\right)=\sum_{i=1}^{3}\lambda_{i}(\omega_{\mathrm{e}i}-\omega_{\mathrm{a}i})^{2}+\sum_{i=1}^{3}\gamma_{i}\left(1-\frac{(\phi_{\mathrm{a}i}^{\mathrm{T}}\phi_{\mathrm{e}i})^{2}}{(\phi_{\mathrm{a}i}^{\mathrm{T}}\phi_{\mathrm{a}i})(\phi_{\mathrm{e}i}^{\mathrm{T}}\phi_{\mathrm{e}i})}\right)\\ \gamma_{i}=\sum_{j=1}^{n}X_{ij}G_{j}/\sum_{j=1}^{n}X_{ij}^{2}G_{j}\quad(i=1,2,3)\\ \gamma_{i}\geq 0\quad(i=1,2,3)\\ \sum_{i=1}^{3}\gamma_{i}=1\end{array}\tag{3}$$

Thus multi-objective optimization problem in Eq. (1) were transformed into the one-dimensional single-objective optimization problem in Eq. (3). The classical 0.618 method was used to solve optimal k_b value.

Given the different contribution of each mode to structural response, the weighting coefficients in Eq. (2) were taken as the participation coefficients of the first 3 modes respectively. In which X_{ij} is the j^{th} component of the i^{th} mode shape vector and G_j is the gravity of the j^{th} mass. Finally, $\gamma_1 = 0.7$, $\gamma_2 = 0.2$ and $\gamma_3 = 0.1$ were taken for the model with infill walls, $\gamma_1 = 0.65$, $\gamma_2 = 0.2$ and $\gamma_3 = 0.15$ were taken for the model without infill walls.

In consideration of the design horizontal shear stiffness of isolation layer was 40800kN/m, and the result from the other researchers (Skinner et al. 1996), the initial iteration interval $[k_{b1}, k_{b2}]$ was taken as $[0.3, 0.5]*10^6$ kN/m, and ε was taken as 0.01. Finally, after several iterations, the actual horizontal stiffness k_b=444720kN/m of the isolation layer of structure with infill walls under ambient vibration was obtained. It is 10.9 times of that in the design case of frequently-occurred earthquake level. The same process was conducted and then the actual horizontal stiffness k_b=438600kN/m without infill walls under ambient vibration was obtained. It is 10.75 times of that in the design case of frequently-occurred earthquake level. These two stiffness values are even greater than the inter-story lateral stiffness values of the 3rd and 4th storey with infill walls.

Comparison of dynamic characteristics of base-isolated structure with and without infill walls when rubber bearings have different shear deformation is shown in Table 3.

Table 3 Dynamic parameters of the base-isolated structure under different cases

<table>
<tr><th colspan="2">Case</th><th>k_b (kN/m)</th><th>ζ_{eq}</th><th>T_1 (s)</th></tr>
<tr><td colspan="2">Base-fixed finite element model with infill walls</td><td>-</td><td>-</td><td>0.320</td></tr>
<tr><td rowspan="2">Ambient excitation</td><td>With infill walls</td><td>444720</td><td><0.05</td><td>0.3344</td></tr>
<tr><td>Without infill walls</td><td>438600</td><td><0.05</td><td>0.3889</td></tr>
<tr><td colspan="2">Frequently-occurred earthquake level($\gamma = 50\%$)</td><td>40800</td><td>0.174</td><td>1.7247</td></tr>
<tr><td colspan="2">Rarely-occurred earthquake level ($\gamma = 250\%$)</td><td>21520</td><td>0.117</td><td>2.3495</td></tr>
</table>

In Table 3, k_b and ζ_{eq} is horizontal equivalent stiffness and equivalent damping ratio of the isolation layer respectively, and T_1 is fundamental period of the base-isolated structure. There is large difference in both k_b and ζ_{eq} with the various shear deformation of rubber bearings. Thus T_1 is totally different under different case.

The k_b values of the structure with and without infill walls are somewhat different. The first reason is the influence of infill walls on structural performance. And the unavoidable error of testing and analysis is probably another reason for this difference.

5. CONCLUSIONS

2 dynamic tests under ambient excitation and modal parameter identification were conducted on a base-isolated RC frame structure before and after the infill walls were constructed. Identified modal parameters are significantly different from the analytical results under design earthquake levels. The main reason is that the actual horizontal stiffness of isolated layer under ambient vibration is difficult to define precisely. Then the structures with and without infill walls were taken as case study, the actual horizontal stiffness of isolation layer under ambient excitation was inversed precisely using the multi-objective optimization method. The results show that the actual horizontal stiffness value is 10.9 times of that under frequently-occurred earthquake level for the case with infill walls, and it is 10.75 times of design value under frequently-occurred earthquake level for the case without infill walls.

In addition, the results also show that the identified damping ratios of two cases under ambient excitation are rather low, damping characteristic of both superstructure and rubber bearings do not have too much difference. So, it is reasonable to treat the base-isolated system as a classically damped system under low level vibration such as the case of ambient excitation and low level earthquake excitation.

REFERENCES

Du, Y.F., Li, H., Spencer, B.F. and Zhao, G.F. (2003), “Real mode superposition method for analysis of seismic response of non-proportionally damped isolated structures”, *Engineering Mechanics,* **20**(4), 24-32.

Han, J.P., Wang, F.X. and Li, H. (2008), “Comparison of modal parameter identification algorithms based on shaking table model test data”, *Journal of Huazhong University of Science and Technology (Urban Science Edition),* **25**(3), 57-60.

Kasai, K. (2011), “Response-controlled structure”, http://eqclearinghouse.cuee.titech.ac.jp/groups/tohoku2011/.

GB50011-2010 (2010), *Code for Seismic Design of Buildings*, Beijing, China.

Mo, Y., Jin, J.M., Du, Y.F. and Cao, B.H. (2008), “A probe in structural form selection for buildings in high-intensity earthquake region--reflection on issues of structural form selection in survey on damages of Wenchuan earthquake on May 12th to architectural structure of buildings in Longnan area”, *Earthquake Resistant Engineering and Retrofitting,* **30**(4), 50-55.

Juang, J.N. (1994), *Applied System Identification,* Prentice-Hall, Englewood Cliffs, New Jersey, USA.

Overschee, P.V. and Moor, B.D. (1996), *Subspace Identification for Linear Systems,* Kluwer Academic Publishers, Boston, USA.

Ren, W.X. and Peng, X.L. (2007), “Baseline dynamic finite element model of Qingzhou cable-stayed bridge”, *Chinese Journal of Computational Mechanics,* **24**(5), 609-613.

Skinner, R.I., Robinson, W.H. and Mcverry, G.H. (1993), *An Introduction to Seismic Isolation,* John Wiley & Sons, New York, USA.

Ventura, C.E., Finn, W.D.L., Lord, J.F. and Fujita, N. (2003), “Dynamic characteristics of a base isolated building from ambient vibration measurements and low level earthquake shaking”, *Soil Dynamics and Earthquake Engineering,* **23**(4), 313-322.

Zhou, F.L. (1997), *Seismic Mitigation Control of Engineering Structures*, Seismological Press, Beijing, China.